

Article

A Study on the Application Possibility of the Vehicle Air Conditioning System Using Vortex Tube

Younghyeon Kim ¹, Seokyeon Im ^{2,*} and Jaeyoung Han ^{3,*}

¹ Department of Mechanical Engineering, Chungnam National University, 99 Daehak-ro, Yuseong-gu, Daejeon 34134, Korea; viny9198@naver.com

² Department of Mechanical and Materials Engineering Education, Chungnam National University, 99 Daehak-ro, Daejeon 34134, Korea

³ School of Mechanical & Automotive Engineering, Youngsan University, 288 Junam-ro, Yongsan-si 50510, Korea

* Correspondence: imsy@cnu.ac.kr (S.I.); hjyt11@ysu.ac.kr (J.H.); Tel.: +82-42-821-7992 (S.I.); +82-055-380-9473 (J.H.); Fax: +82-42-821-8732 (S.I.); +82-55-380-9249 (J.H.)

Received: 9 August 2020; Accepted: 7 October 2020; Published: 8 October 2020



Abstract: Since refrigerants applied to vehicle air conditioning systems exacerbate global warming, many studies have been conducted to supplement them. However, most studies have attempted to maximize the efficiency and minimize the environmental impact of the refrigerant, and thus, an air conditioning system without refrigerant is required. The vortex tube is a temperature separation system capable of separating air at low and high temperatures using compressed air. When applied to an air conditioning system, it is possible to construct an eco-friendly system that does not use a refrigerant. In this paper, various temperature changes and characteristics of a vortex tube were identified and applied to an air conditioning system simulation device. Additionally, an air conditioning system simulation device using indirect heat exchange and direct heat exchange methods was constructed to test the low-temperature air flow rate (y_c), according to the temperature and pressure. As a result of the experiment, the temperature of the indirect heat exchange method was found to be higher than the direct heat exchange method, but the direct heat exchange method had low flow resistance. As a result, the direct heat exchange method can easily control the temperature according to the pressure and the low-temperature air flow rate (y_c). Therefore, it was judged that the direct heat exchange method is more feasible for use in air conditioning systems than the indirect heat exchange method.

Keywords: vortex generator; vortex tube; temperature separation; the low-temperature air flow ratio (y_c), inlet pressure (P_i)

1. Introduction

With rapid industrialization, the share of fossil fuels has increased significantly from the beginning of the industrial revolution to the present, and as means of transportation and efficient heating and cooling systems have been developed, more environmental pollution has been produced. Furthermore, the excessive use of refrigerant has caused environmental problems such as ozone layer destruction and global warming, and the ripple effects are accelerating. Accordingly, restrictions on the use of CFC (Chloro Fluoro Carbon)-based refrigerants have been strengthened, and R134a has been developed as an alternative. This refrigerant has been applied to facilities such as automobile air conditioning systems and household refrigerators. However, while R134a has an ozone depletion index of 0, its global warming index of 1430 is insufficient to compensate for environmental problems [1,2]. As an alternative to solve the problems associated with freon (CFC) used as a refrigerant in automobiles, research has been actively conducted, where one possible measure is the vortex tube [3].

The vortex tube was discovered by Ranque in 1928 and has since become widely promoted to the academic community by Hilsch [4,5]. Thereafter, modeling studies were conducted by Fulton, Stephan, Deissler and Permuter, Kassner, Upendra, and Gao et al. for energy separation, and models proposed by Fulton and Kassner have been widely accepted [6–11]. Hilsch et al. experimented to find nozzle diameters and low-temperature exit conditions for three cases of tube radii of 4.6 mm, 9.6 mm, and 17.6 mm. Westley et al. conducted a study on vortex tube dimensional conditions to find the ratio of the tube area of the low-temperature air outlet area to the tube area of the nozzle's total area to spray compressed air into the tube [12]. Hartnett and Eckert et al. measured the tube velocity, pressure, and temperature distribution through experiments and found that the vortex tube had a high wall temperature and a low central temperature [13]. Takanama et al. designed the shape of a vortex tube with high energy efficiency by researching the relationship between the temperature and velocity distribution of air flowing in the vortex internal production chamber and the dimensions of the tube, nozzle, and low-temperature outlet orifice [14]. Comassar and Stepan et al. presented a single-flow vortex tube to evaluate the energy separation performance and confirmed that the counter-flow vortex tube performance was higher than the single-flow vortex tube [15,16]. Frohlingsdorf et al. analyzed energy separation and flow in a Ranque–Hilsch vortex tube using CFX, shear stress, and axial symmetry models [17]. Smith Eiamsa-ard et al. performed a thermal separation simulation of a Ranque–Hilsch vortex tube in a finite volume approach using a standard turbulence model and a logarithmic stress model (ASM) [18]. Skye et al. compared the performance predicted by the CFD model with commercial vortex tube experimental data and confirmed the industrial applicability of vortex tubes [19].

Until recently, studies on the industrial use of vortex tubes are ongoing, and experimental analysis of vortex tube energy separation phenomena and comparative analysis through models are continuously being studied [20–23]. B.E. Mtopi Fotso et al., and others, showed modeling and thermal analysis of solar generators equipped with vortex tubes for hybrid vehicles, showing the application of vortex tubes to vehicles [24]. Additionally, Hitesh R. Thakare et al. performed a technical and economic evaluation of the vortex tube's industrial applications to show that the industrial use of vortex tubes is advantageous for shortening production cycles [25].

In this study, the vortex tube was found to be eco-friendly because it does not require a refrigerant; and because it is sufficiently applicable to air conditioning systems in the future automobile field, a study was conducted to integrate a vortex tube into a vehicle air conditioning system. The experiment was performed by dividing it into two parts: an indirect heat exchange method and a direct heat exchange method. In particular, among the factors affecting the energy separation of the vortex tube, the temperature is controlled by controlling the supply pressure (P_i), the nozzle area ratio (S_n), and the number of nozzle holes (N_h) of the vortex tube generator, and the low-temperature air flow rate (y_c) is controlled using a throttle valve. We obtained the experimental data for the four basic and influential characteristics in the characteristic experiment, and based on this, analyzed the optimum temperature characteristics by installing them in heat exchangers of different shapes using the indirect and direct methods.

2. Experimental Approach

2.1. Principle of Vortex Tube

The vortex tube is an energy separation device that separates compressed air into hot and cold air samples without chemical reaction or combustion. The vortex tube has a simple structure, but the cause and phenomenon of energy separation are complicated. In general, Fulton's theory describing the domains of free vortex and forced vortex is accepted. According to the theory, compressed fluid forms a free vortex with high velocity at the tangential nozzle of the tube.

$$wr^2 = \text{const.} \quad (1)$$

At this time, as the flow proceeds toward the throttle valve, the free vortex is the result of friction between the fluid layers, and a forced vortex is formed in the center of the tube.

$$w = \text{const.} \quad (2)$$

Due to this change in flow type, momentum transfer occurs from the center of the tube to the wall, and the center of the vortex is cooled more than the outside. However, to achieve energy balance, heat is transferred to the inner layer; however, since the momentum transfer is greater than the transfer of heat, the outside air temperature rises as does the stagnant temperature, and air is discharged through the throttle valve as a high-temperature flow. At this time, the fluid inside drops to a lower temperature by losing momentum greater than the received thermal energy, and becomes a low-temperature flow with temperature lower than the inlet temperature; this air is discharged to the outside through the low-temperature outlet orifice. Figures 1 and 2 clearly show the phenomenon of this vortex tube [26]. What is shown in the vertical direction in Figure 1 is a visual representation of the force magnitude in the vortex tangent direction.

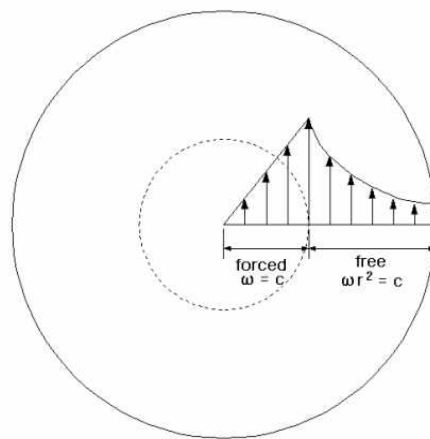


Figure 1. Cross-section of the vortex tube in the “free” and “forced” vortex flow.

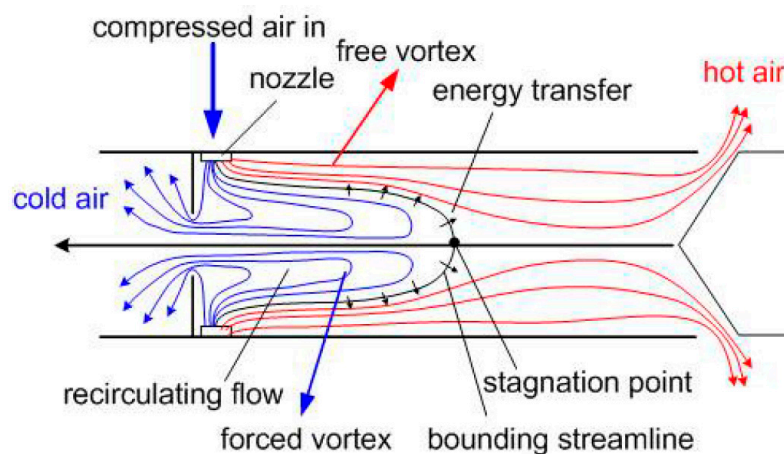
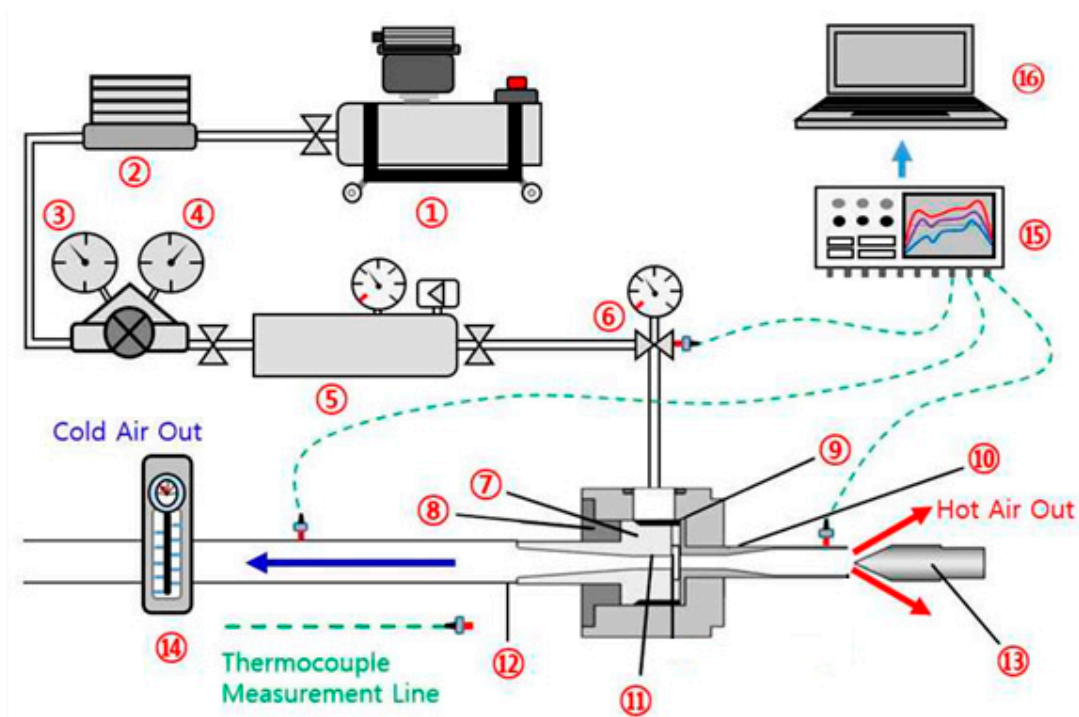


Figure 2. Supposed flow pattern and energy flow in the counter flow type.

2.2. Setup of Feasibility Study

In this study, the vortex tube device was applied to a vehicle air conditioning system. Therefore, through a basic experiment with an actual manufactured vortex tube, it was confirmed whether energy separation had been properly performed; also, the number of nozzle holes (N_h) of the vortex generator was changed according to the supply pressure (P_1) to change the temperature according to

the low-temperature airflow ratio (y_c). Schematics of the basic experimental device and the actual experimental device are shown in Figures 3 and 4.



① Compressor	② Air Dryer	③ Pressure regulator	④ Air filter
⑤ Air surge	⑥ Check valves	⑦ Vortex generator	⑧ Holder
⑨ Nozzle	⑩ Sleeve	⑪ Orifice	⑫ Vortex tube
⑬ Throttle valve	⑭ Air flowmeter	⑮ Data logger	⑯ Lap top

Figure 3. Schematic diagram of the vortex tube system.

The specifications of the vortex tube produced in the experiment are shown in Table 1. The air conditioning system to be applied to the experiment was divided into two types: an indirect heat exchange method and a direct heat exchange method.

Table 1. Dimension of the vortex tube.

Parameter	Value	Unit
Tube length (L)	128	mm
Inlet diameter of vortex tube (D)	9.8	mm
Inner diameter of nozzles (D_n)	1, 1.2, 1.4, 1.7, 2.1	mm
Diameter of cold end orifice (d_c)	6	mm
Number of nozzle holes (N_h)	4, 5, 6, 7, 8	-
Nozzle area ratio (S_n)	0.142	-

Compressed air that has undergone energy separation through the vortex tube first controls the temperature through a low-temperature and high-temperature valve, and this air is moved into the chamber through an indirect heater core where heat exchange is performed using a direct air conditioning filter. The temperature is measured. The heater core of the indirect heat exchanger used

in the experiment is shown in Figure 5; the air conditioning filter of the direct heat exchanger is shown in Figure 6.



Figure 4. Photograph of the experimental apparatus for the vortex tube.



Figure 5. Indirect type heater core.

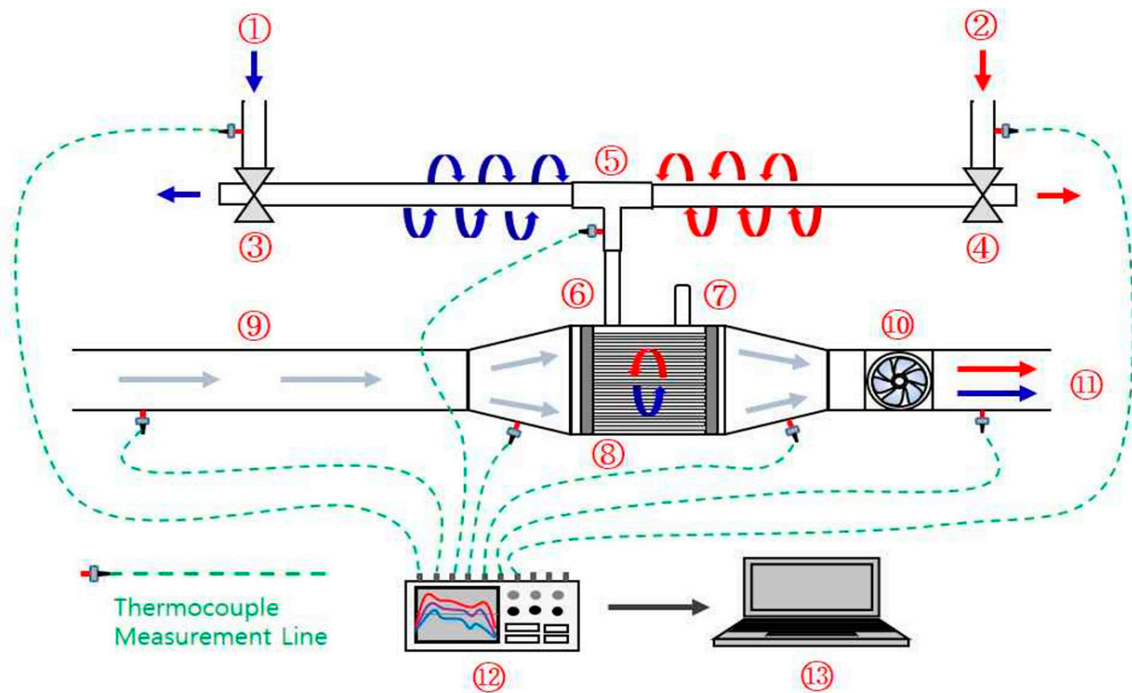


Figure 6. Direct type air conditioning filter.

2.3. Experimental Apparatus

Figures 7 and 8 show the schematic and actual experimental device for the indirect heat exchanger. Figures 9 and 10 show a schematic of the direct heat exchange method and an actual experimental device. Configurations of the experimental device for the vortex tube can be largely divided into three types: a supply unit that supplies compressed air, a test unit that performs temperature separation experiments, and a control unit that controls the system. The supply section consists of an air compressor, air dryer, air surge tank, and pressure regulator, which supplies compressed air. The test section consists of a vortex tube and a throttle valve, thermocouple, pressure gauge, flow meter, etc., that can control the low-temperature air flow rate (y_c). The control part is composed of a part that controls pressure and flow rate and a part that checks data from each temperature sensor. The air entering the inlets (shown in Figures 7 and 9) is hot and cold air separated through the vortex tube; this air is supplied to each inlet. Table 2 shows the specifications of the device used in the experiment.

The compressed air produced by the compressor enters the surge tank. After enough air is present in the surge tank, it passes through the filter and is supplied to the vortex tube inlet. This phenomenon is a process that is conducted to catch the pulsation of the air generated by the compressor, and the following method was used to reduce the experimental error. Then, the supplied air passes through the vortex generator, and the vortex is generated inside the experimental apparatus. The generated vortex induces an energy separation phenomenon in the tube structure, and air separates into hot air and cold air and is discharged. Each type of air is then heat exchanged through the heater core. The air that has undergone heat exchange and the outside air are mixed in the chamber; according to the flow of the air, the experiment was performed by dividing it into indirect and direct methods. If there was no difference of 0.1 °C for 100 s, the temperature was determined to be in a normal state, and the corresponding temperature was measured. In addition, the reliability of the experimental results was secured through repeated experiments.



① T _c inlet air	⑤ T _c to T _h Connection	⑨ Inlet air
② T _h inlet air	⑥ Heater core inlet	⑩ Fan
③ T _c 3way valve	⑦ Heater core outlet	⑪ Outlet air
④ T _h 3way valve	⑧ Heater core	⑫ Data logger
		⑬ Lap top

Figure 7. Schematic diagram of the indirect heater core.

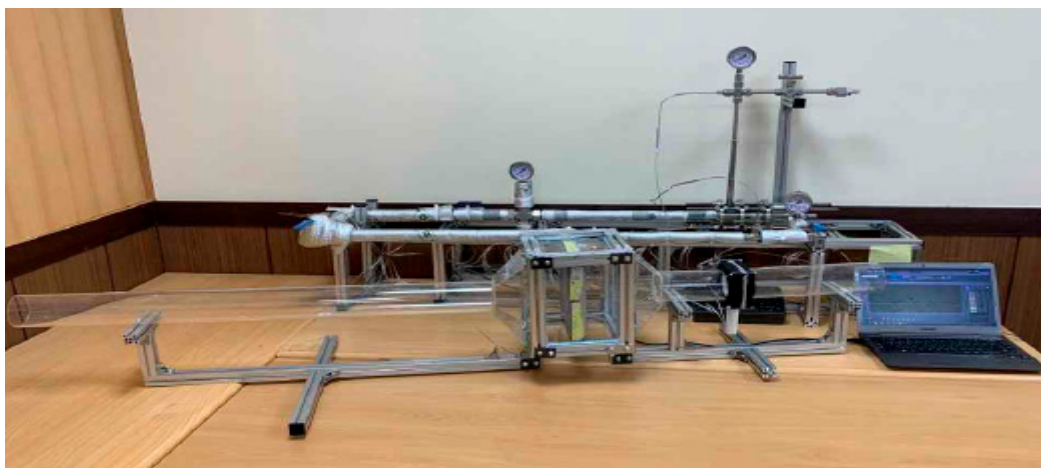
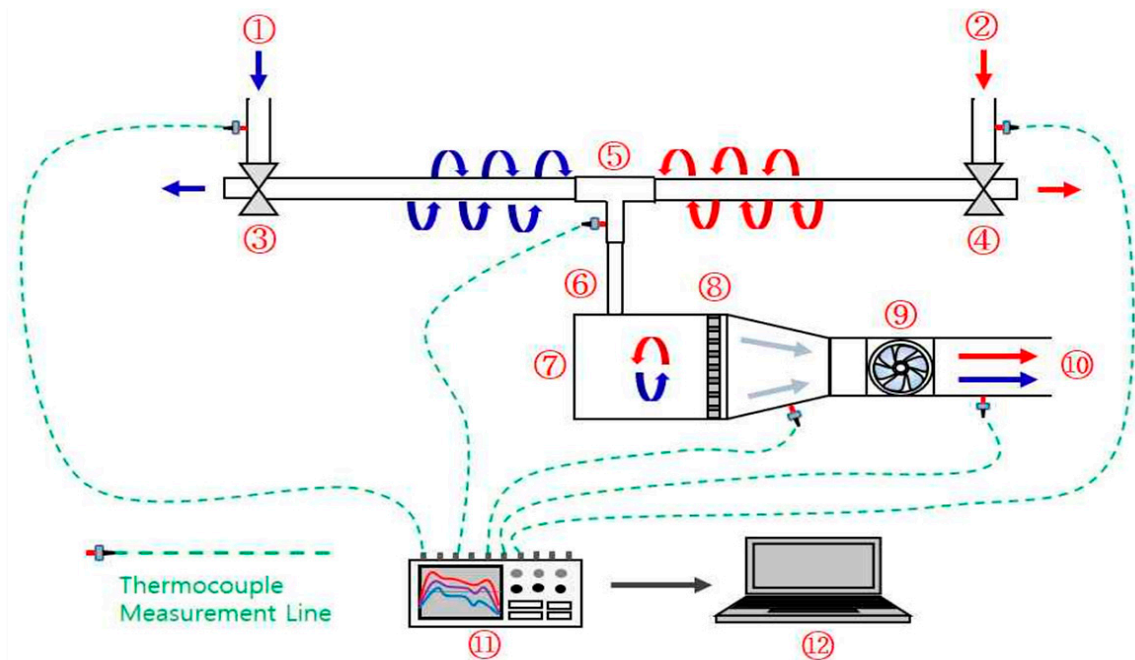


Figure 8. Photograph of an indirect experimental device with a heater core.



① T _c inlet air	⑤ T _c to T _h Connection	⑨ Fan
② T _h inlet air	⑥ Chamber inlet	⑩ Outlet air
③ T _c 3way valve	⑦ Chamber	⑪ Data logger
④ T _h 3way valve	⑧ Air conditioning filter	⑫ Lap top

Figure 9. Schematic diagram of the direct air conditioning filter.

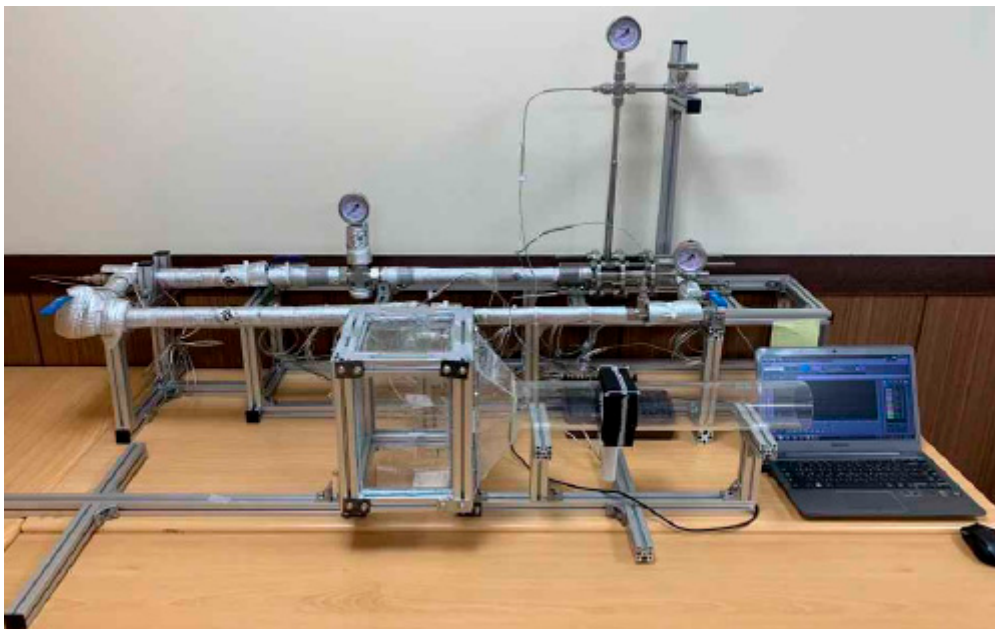


Figure 10. Photograph of the direct experimental device with air conditioning filter.

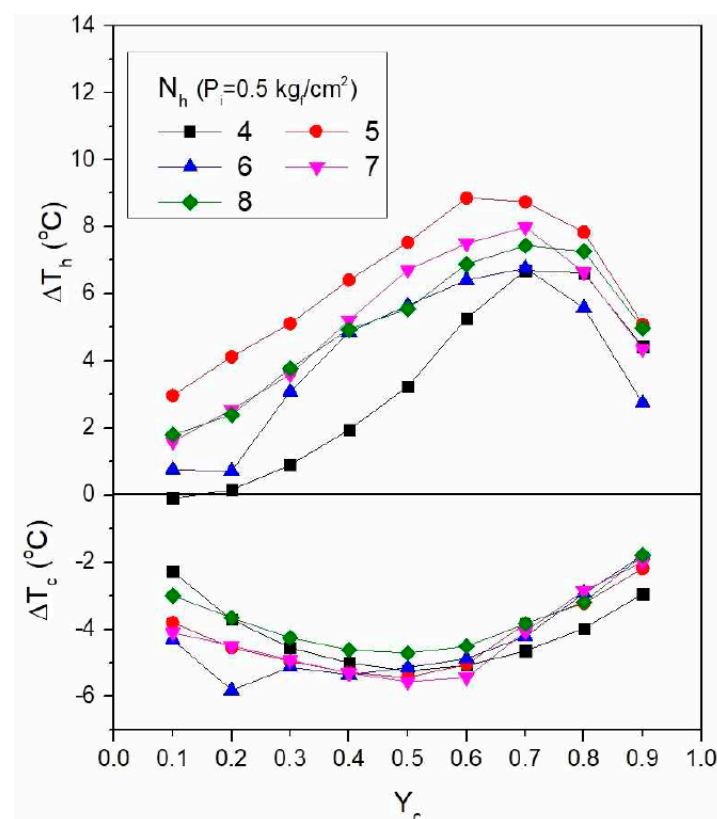
Table 2. Range and uncertainly of the equipment used in the experiment.

Instrument	Model	Range	Uncertainly
Graphtec	GL 840 Midi Logger	-	±0.5%
Thermo-couple	K-type	−100 to 650 °C	±2.5 °C
Pressure sensor	Dream31 (A-type) Dream	−1 to 6 bar	±1.5%
Gas regulator	Renown	0–6 bar	±2.0%
Air compressor	Renown	20 HP	-
Air surge tank	Renown	280 L	-

3. Results and Discussion

3.1. Temperature Change According to Pressure and Generator Nozzle

The temperature change according to the pressure in the vortex tube device and the number of nozzles of the generator was investigated. The nozzle area ratio of $S_n = 0.142$ was set using a commonly known standard. The nozzle area ratio is the standard of the vortex tube that is set to best separate high temperature air. In addition, since the vortex formed in the vortex tube varies depending on the inlet supply pressure, the experiment was performed between $P_i = 0.5 \text{ kgf/cm}^2$ and $P_i = 5.0 \text{ kgf/cm}^2$ at $P_i = 0.5 \text{ kgf/cm}^2$ intervals. For each experiment, the high-temperature air temperature difference ΔT_h and the low-temperature air temperature difference ΔT_c at low temperature air flow rate (y_c) = 0.1~1.0 were measured. Results are shown in Figures 11–20.

**Figure 11.** Temperature differences ΔT_h and ΔT_c according to inlet pressure (P_i) 0.5 kgf/cm².

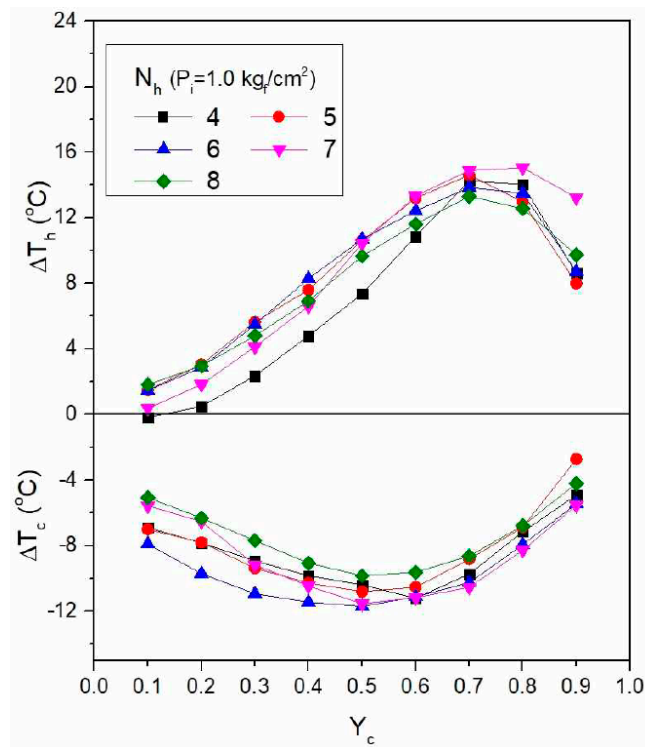


Figure 12. Temperature differences ΔT_h and ΔT_c according to inlet pressure (P_i) 1.0 kgf/cm².

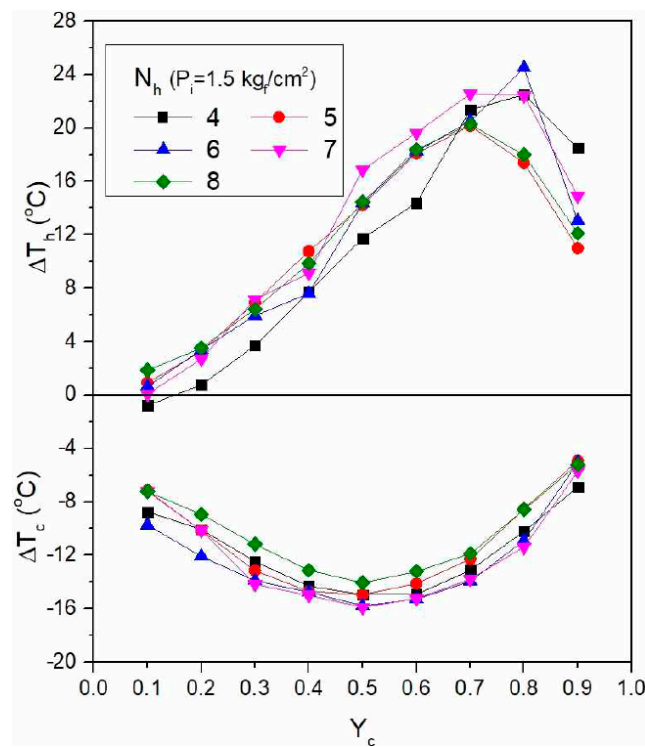


Figure 13. Temperature differences ΔT_h and ΔT_c according to inlet pressure (P_i) 1.5 kgf/cm².

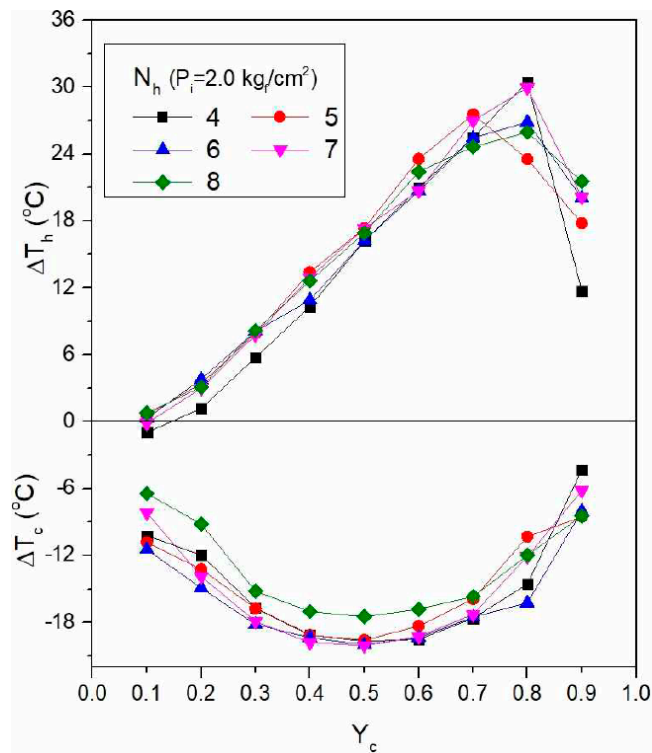


Figure 14. Temperature differences ΔT_h and ΔT_c according to inlet pressure (P_i) 2.0 kgf/cm².

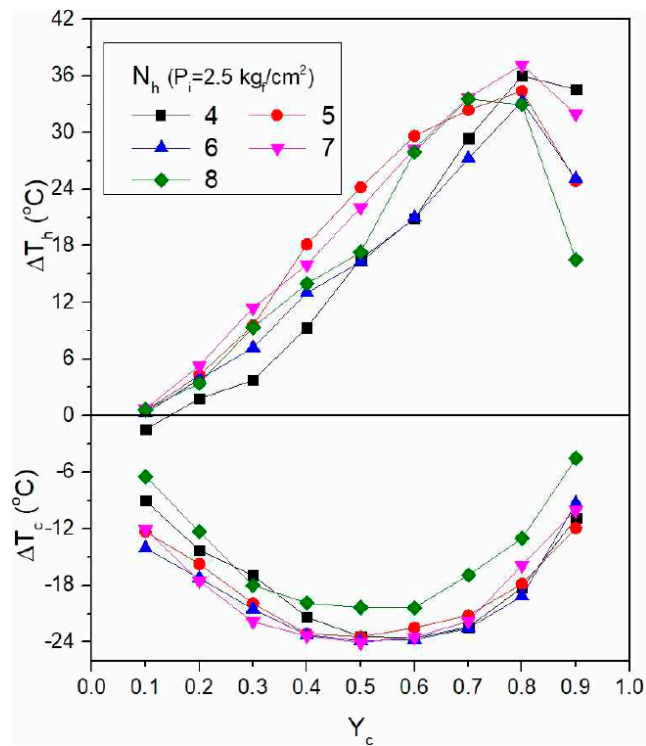


Figure 15. Temperature differences ΔT_h and ΔT_c according to inlet pressure (P_i) 2.5 kgf/cm².

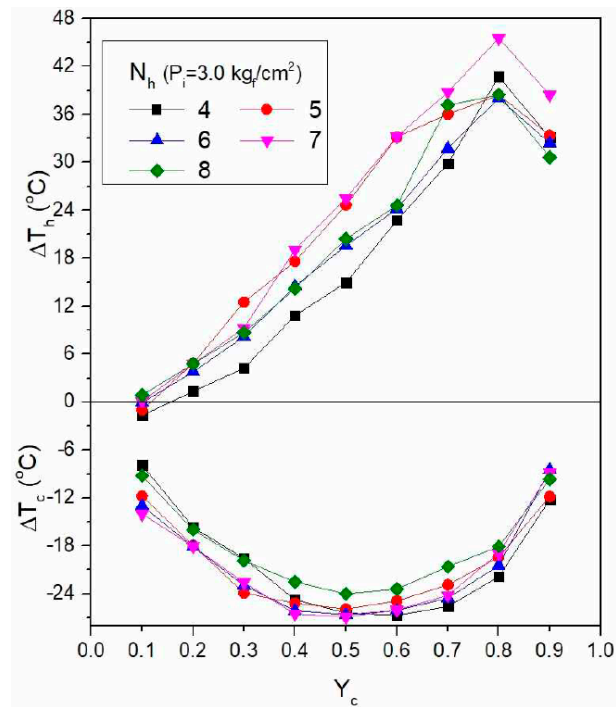


Figure 16. Temperature differences ΔT_h and ΔT_c according to inlet pressure (P_i) 3.0 kgf/cm².

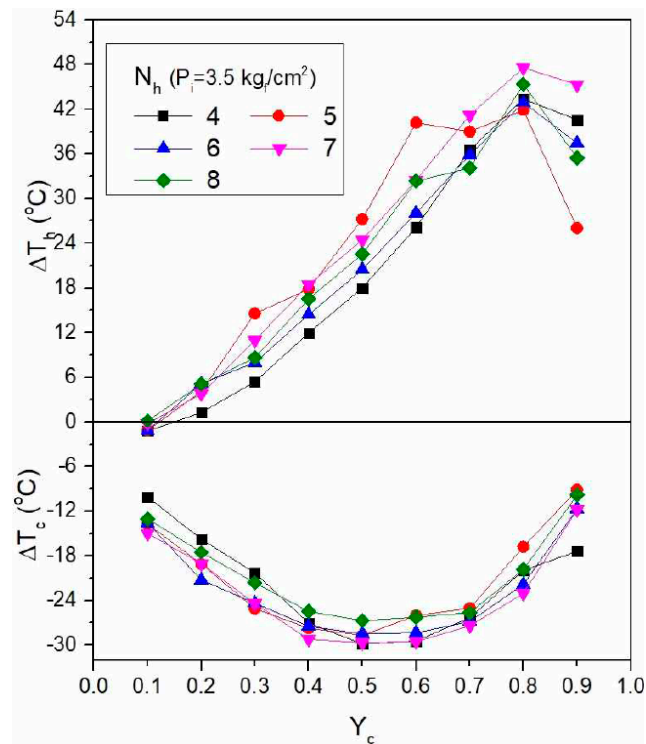


Figure 17. Temperature differences ΔT_h and ΔT_c according to inlet pressure (P_i) 3.5 kgf/cm².

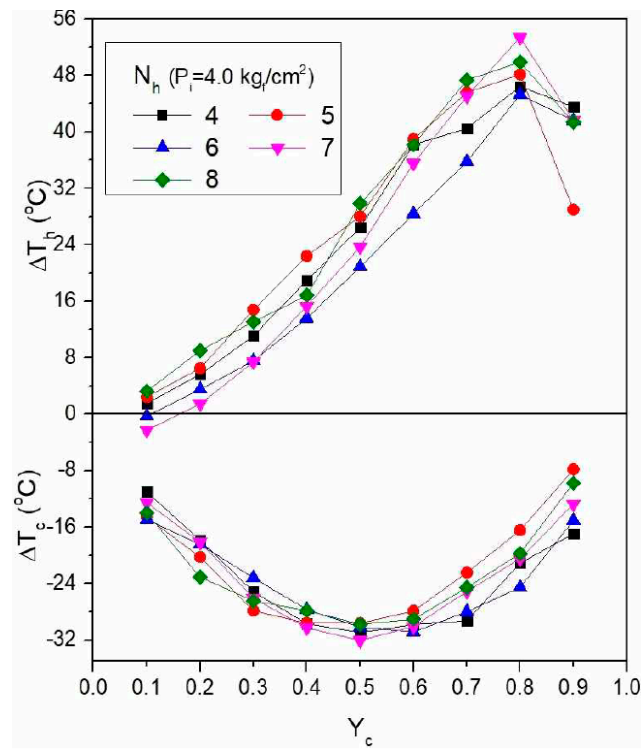


Figure 18. Temperature differences ΔT_h and ΔT_c according to inlet pressure (P_i) 4.0 kgf/cm².

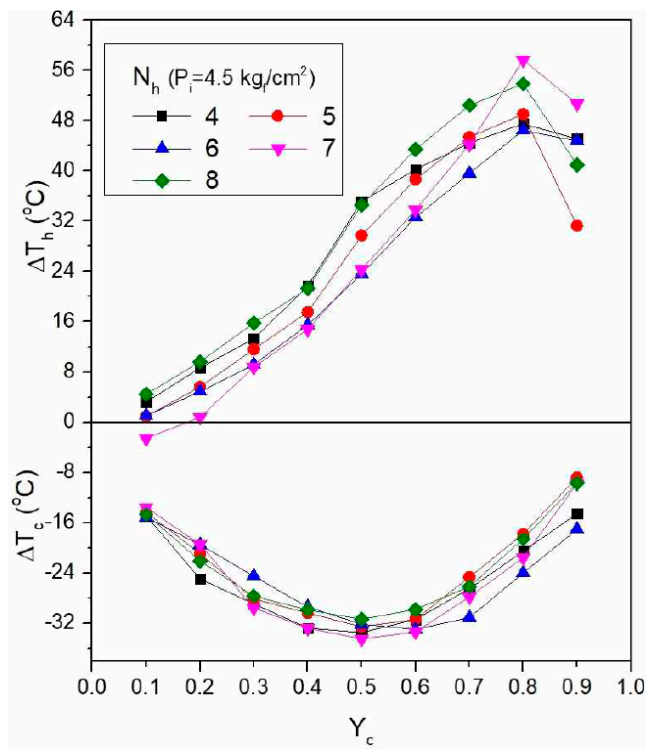


Figure 19. Temperature differences ΔT_h and ΔT_c according to inlet pressure (P_i) 4.5 kgf/cm².

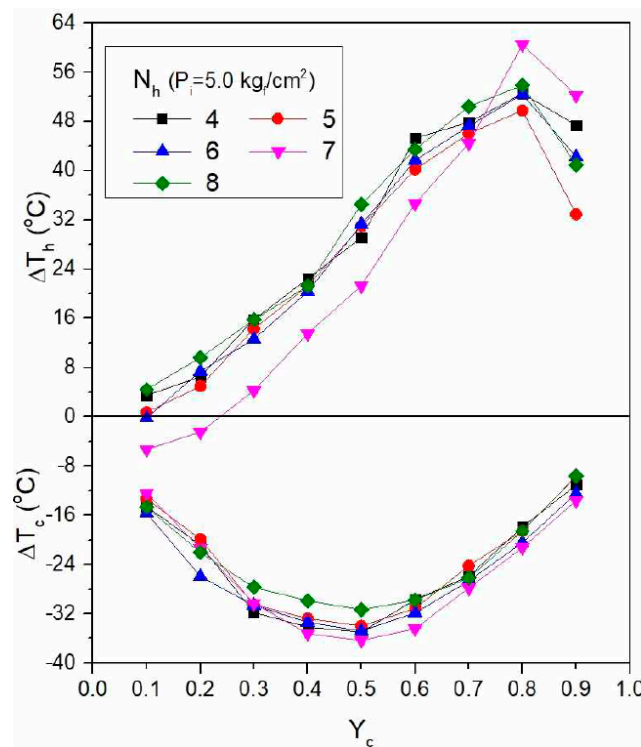


Figure 20. Temperature differences ΔT_h and ΔT_c according to inlet pressure (P_i) 5.0 kgf/cm².

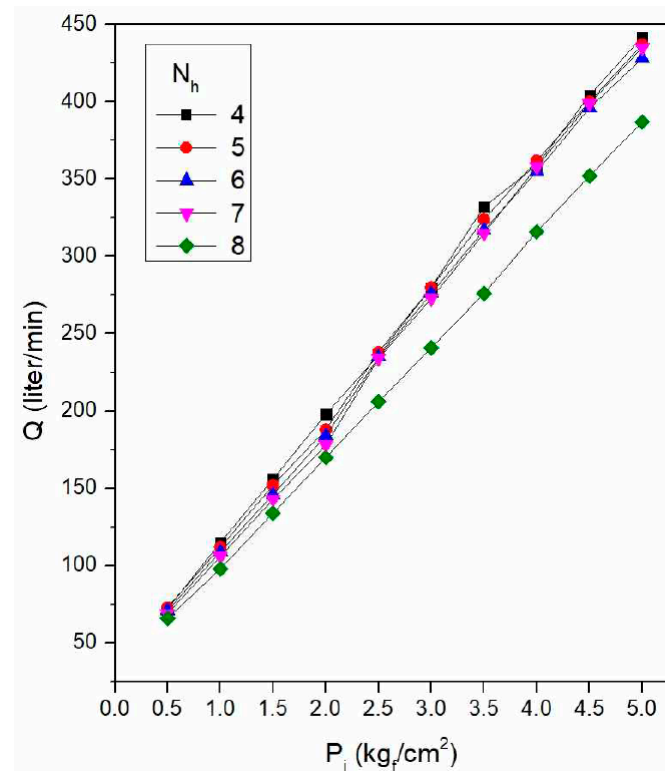
According to the experimental results, it was confirmed that ΔT_h showed the highest high-temperature air from $y_c = 0.6$ to 0.8 at high temperatures, and $y_c = 0.8$ in the case of $\Delta T_{h, \max}$ as the pressure increased. In the case of low temperature, ΔT_c showed the maximum low-temperature air from $y_c = 0.4$ to 0.6 , and in the case of $\Delta T_{c, \max}$ in the same case as the high temperature, $y_c = 0.5$. As a result of these experiments, when the throttle valve on the high-temperature outlet is closed, y_c increases and the flow cross-sectional area of the high-temperature outlet decreases. Therefore, the air at the high-temperature outlet flows back to the relatively low-temperature outlet, and the central flow becomes smooth. Additionally, when y_c relatively decreases, the flow cross-sectional area of the high-temperature outlet becomes wider, and ΔT_c tends to increase because the stagnation point in the vortex tube moves more toward the high-temperature outlet than it does when y_c increases. It was judged that ΔT_h and ΔT_c increased because of active energy separation due to increases in momentum transfer between the central flow and the flow near the wall due to the change in y_c . Through the experiments, it was found that ΔT_h and ΔT_c increased in a similar manner as the inlet pressure (P_i) flowing into the vortex tube increased. As the inlet pressure increased, the flow rate increased, and so the energy loss of the flow decreased, regardless of the number of nozzles, and the energy separation phenomenon became relatively large. This experiment trend showed similar tendencies of low-temperature outlet flow rate and entire pressure section, just as in Stephan [7]. Table 3 shows the $\Delta T_{h, \max}$ and $\Delta T_{c, \max}$ values of y_c , and the number of nozzles depending on the pressure; in the case of T_h , it can be seen that the number of nozzles varied from inlet pressure $P_i = 0.5$ to 2.0 kgf/cm². However, after $P_i = 2.0$ kgf/cm², it can be seen that the number of nozzles appears constant; in the case of T_c , the number of nozzles seems to change at $P_i = 1.0$ kgf/cm². Overall, in the case of T_h , the temperature was highest at $y_c = 0.8$, and the nozzles were found to be efficient when they had seven holes. T_c was found to have its lowest temperature at $y_c = 0.5$, and the number of nozzles was found to be efficient at seven.

Table 3. $T_{h, \max}$ and $T_{c, \max}$ of y_c and nozzle holes depending on the pressure.

P_i	$T_{h, \max}$	y_c	N_h	$T_{c, \max}$	y_c	N_h
0.5	8.86 °C	0.6	5 hole	−5.57 °C	0.5	7 hole
1.0	15.06 °C	0.8	7 hole	−14.17 °C	0.5	6 hole
1.5	24.51 °C	0.8	6 hole	−15.90 °C	0.5	7 hole
2.0	30.42 °C	0.8	4 hole	−20.08 °C	0.5	7 hole
2.5	37.17 °C	0.8	7 hole	−24.06 °C	0.5	7 hole
3.0	45.55 °C	0.8	7 hole	−26.90 °C	0.5	7 hole
3.5	47.61 °C	0.8	7 hole	−29.66 °C	0.5	7 hole
4.0	53.38 °C	0.8	7 hole	−32.05 °C	0.5	7 hole
4.5	57.70 °C	0.8	7 hole	−34.46 °C	0.5	7 hole
5.0	60.51 °C	0.8	7 hole	−36.33 °C	0.5	7 hole

3.2. Discharge Flow Rate and Temperature Difference between $\Delta T_{h, \max}$ and $\Delta T_{c, \max}$ According to Pressure

As an initial experiment, we tried to determine the total flow rate according to the supply pressure. The table that summarizes the data according to the number of nozzles is shown in Figure 21.

**Figure 21.** Total discharge flow rate of intake air pressure by the number of nozzles.

The nozzle cross-section (S_n) of the generator was selected as a high-temperature type. As a result of experiments on low-temperature and high-temperature type nozzles, the temperature difference was found not to be large in the low-temperature region, but showed a difference of about 8 °C in the high-temperature region. This phenomenon is considered to be due to an increase in flow resistance because the cross-sectional area of the high-temperature nozzle has a smaller area ratio than that of the low-temperature nozzle. This can be seen in the nozzle cross-section experiment [27]. The purpose of this experiment was to determine the conditions for effective temperature separation characteristics with minimal flow. Like in the basic experiment, the supply pressure between $P_i = 0.5 \text{ kgf/cm}^2$ and $P_i = 5.0 \text{ kgf/cm}^2$ to the vortex generator was set at the interval of $P_i = 0.5 \text{ kgf/cm}^2$. In the experiment, it can be seen that the discharge flow rate increased proportionally as the inlet supply

pressure increased, regardless of the number of generator nozzles. Under the same pressure condition, the number of nozzles tends to slightly increase as the size of the nozzle decreases, which means that when the generator's nozzle cross-section (S_n) is the same, as the number of generator nozzles decreases, the nozzle inner diameter (D_n) of the nozzle cross-section (S_n) increases. Therefore, it is considered that the total discharge flow rate increases because the flow resistance of compressed air, through which the supply pressure flows through the generator nozzle, decreases. From the experimental results, according to the number of nozzles and the supply pressure of the vortex generator, the maximum high-temperature air temperature difference ($\Delta T_{h, \max}$) and the maximum low-temperature air temperature difference ($\Delta T_{c, \max}$) under each condition are determined and shown in Figure 22.

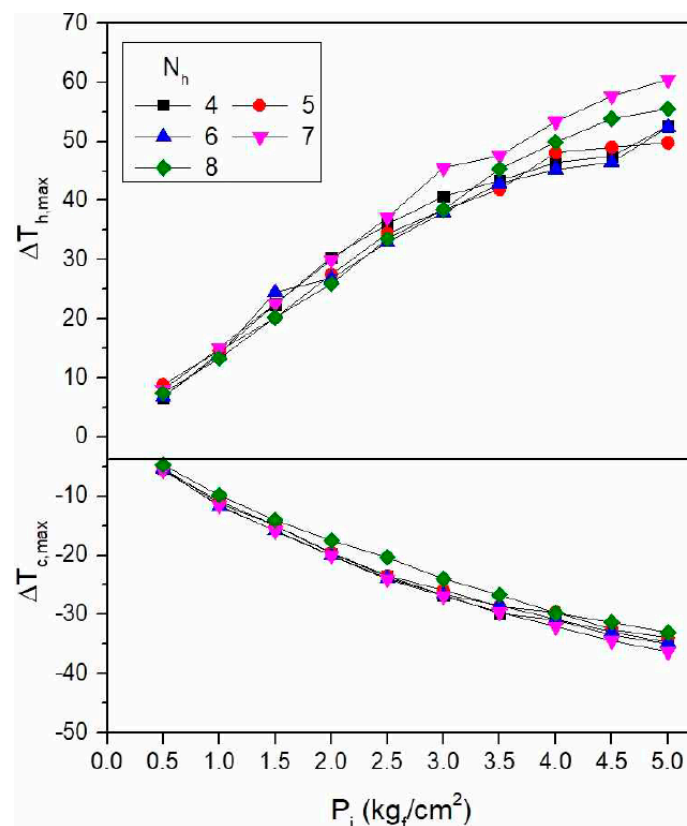


Figure 22. Temperature difference $\Delta T_{h, \max}$ and $\Delta T_{c, \max}$ according to the number of nozzle holes.

As a result of the experiment, most high-temperature and low-temperature air temperature separation characteristics showed good efficiency under certain conditions in the case of the seven nozzles, but there was not a large difference in temperature. Furthermore, it can be seen that for the temperature separation characteristic, the maximum high-temperature air temperature difference ($\Delta T_{h, \max}$) and the maximum low-temperature air temperature difference ($\Delta T_{c, \max}$) changed significantly as the supply pressure increased. The high-temperature air of the seven nozzles with high efficiency changed from 7.99 °C when the maximum hot air temperature difference ($\Delta T_{h, \max}$) $P_i = 0.5$ kgf/cm² to 60.51 °C when $P_i = 5.0$ kgf/cm², and showed a temperature difference of 52.52 °C. The low temperature air varied from −5.57 °C when the maximum low temperature air temperature difference ($\Delta T_{c, \max}$) $P_i = 0.5$ kgf/cm² to −36.33 °C when $P_i = 5.0$ kgf/cm², and showed a temperature difference of 30.76 °C. The result of this experiment provides information for the application of a vehicle air conditioning system. Current air conditioning systems for vehicles have values of $P_i = 2.5$ kgf/cm² to $P_i = 5.0$ kgf/cm², where the temperature change is constant in a vehicle with an air conditioning system using a refrigerant. Based on the experimental results, it is considered that controlling the flow

rate and temperature values required for heating and cooling by checking the discharge flow rate and the temperature difference between the hot and cold parts is a key point.

3.3. Temperature Control of Indirect Heat Exchange Method According to Pressure

To measure the temperature of the indirect heat exchanger, between $P_i = 0.5 \text{ kgf/cm}^2$ and $P_i = 5.0 \text{ kgf/cm}^2$ and $P_i = \text{kgf/cm}^2$ were set based on the number of nozzles of the vortex generator, which was the most efficient in the basic experiment. In the high-temperature type device, the experiment was conducted at a section $y_c = 0.6$ to 0.8 at a point where the efficiency of the low-temperature air flow rate (y_c) was good; the experiment was conducted at $y_c = 0.4$ to 0.6 for a section of low-temperature type. Figure 23 shows these results graphically. As in the basic experiment, it can be seen that the vortex tube increases in efficiency with increasing pressure. In the experiment, the value of T_{aoc} ($^{\circ}\text{C}$) is the point at which the temperature of both the vortex tube cold and hot outlets passes through the heater core. Additionally, the value of ΔT_{ac} ($^{\circ}\text{C}$) was expressed by measuring the temperature of the flow flowing into the front and rear ends of the chamber surrounding the heater core. In the case of T_{aoc} ($^{\circ}\text{C}$), the temperature was measured by comparing the low-temperature air flow rate (y_c) of the flow. In the low-temperature region, the temperature difference of T_{aoc} ($^{\circ}\text{C}$) was not large, but it was $21.84 \text{ }^{\circ}\text{C}$ when $P_i = 0.5 \text{ kgf/cm}^2$ at $y_c = 0.6$, where the efficiency was best in proportion to the discharge flow rate, and when $P_i = 5.0 \text{ kgf/cm}^2$. The temperature difference changed to $9.87 \text{ }^{\circ}\text{C}$ and showed a maximum temperature difference of $11.97 \text{ }^{\circ}\text{C}$. The value of ΔT_{ac} ($^{\circ}\text{C}$) was also measured using the low-temperature airflow ratio (y_c), and the temperature difference was similar to T_{aoc} ($^{\circ}\text{C}$). The value of ΔT_{ac} ($^{\circ}\text{C}$) showed values of $-0.03 \text{ }^{\circ}\text{C}$ when $P_i = 0.5 \text{ kgf/cm}^2$ at $y_c = 0.6$, and $-11.92 \text{ }^{\circ}\text{C}$ when $P_i = 5.0 \text{ kgf/cm}^2$, resulting in a maximum temperature difference of $11.95 \text{ }^{\circ}\text{C}$. Through this, the low-temperature measurement of the indirect heat exchange method according to the pressure, $y_c = 0.5$ was excellent in the basic experiment, but when heat exchange was performed, the resulting value of $y_c = 0.6$, which indicates a relatively large discharge flow rate due to flow rate resistance, was the best.

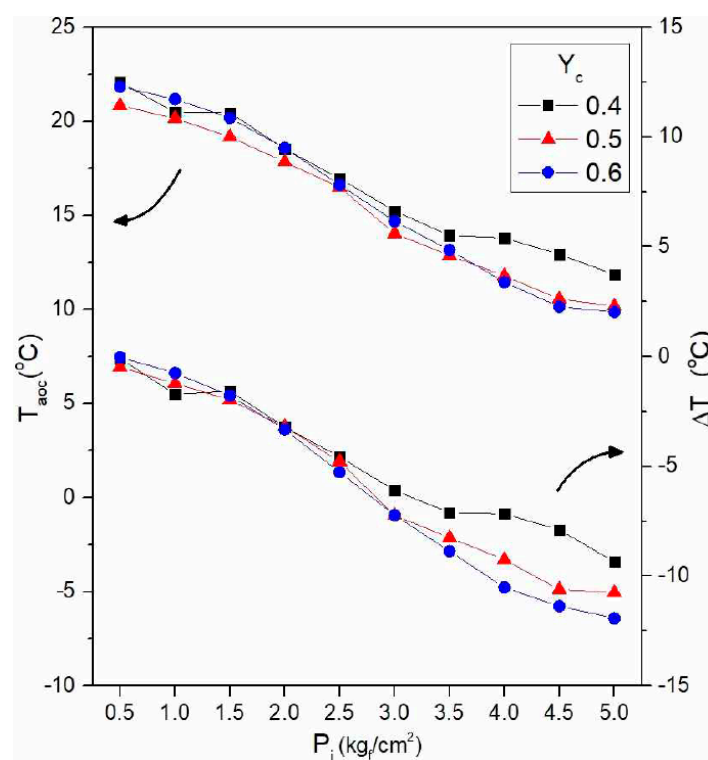


Figure 23. Indirect heat exchange method of ΔT_{aoc} and ΔT_{ac} according to pressure.

As can be seen in Figure 24, the temperature difference was higher in the high-temperature region than in the low-temperature region. At $y_c = 0.8$, the highest temperature of T_{aoc} ($^{\circ}\text{C}$), when $P_i = 0.5 \text{ kgf/cm}^2$, was $23.00 \text{ }^{\circ}\text{C}$; when $P_i = 5.0 \text{ kgf/cm}^2$, this value changed to $38.79 \text{ }^{\circ}\text{C}$, showing a maximum temperature difference of $15.79 \text{ }^{\circ}\text{C}$. The value of ΔT_{ac} ($^{\circ}\text{C}$) was measured through the low-temperature airflow ratio (y_c), and the temperature difference had a result somewhat similar to that for T_{aoc} ($^{\circ}\text{C}$). At $y_c = 0.8$, $P_i = 0.5 \text{ kgf/cm}^2$ showed a difference of $0.02 \text{ }^{\circ}\text{C}$, and $P_i = 5.0 \text{ kgf/cm}^2$ showed a difference of $15.95 \text{ }^{\circ}\text{C}$; the pressure difference resulted in a maximum temperature difference of $15.93 \text{ }^{\circ}\text{C}$. However, in the high-temperature region of the indirect heat exchange method, it was confirmed that, unlike in the case at low temperature, the influence of pressure was large. In the case of $y_c = 0.8$, it can be seen that the discharge flow rate is low and the temperature change is small until the pressure becomes $P_i = 3.0 \text{ kgf/cm}^2$; the pressure changes significantly after $P_i = 3.0 \text{ kgf/cm}^2$. Through these experiments, it is thought that the reaction rate of the heat exchanger will be higher than between $y_c = 0.7$ and 0.8 in the indirect heat exchange method when $y_c = 0.6$, which has a constant temperature change and a large discharge flow rate. Therefore, as a result of confirming the temperature difference according to the low-temperature air flow rate (y_c) through an indirect heat exchange method that changes according to the pressure, it was determined that a value of $y_c = 0.6$ is suitable for regions of both low temperature and high temperature.

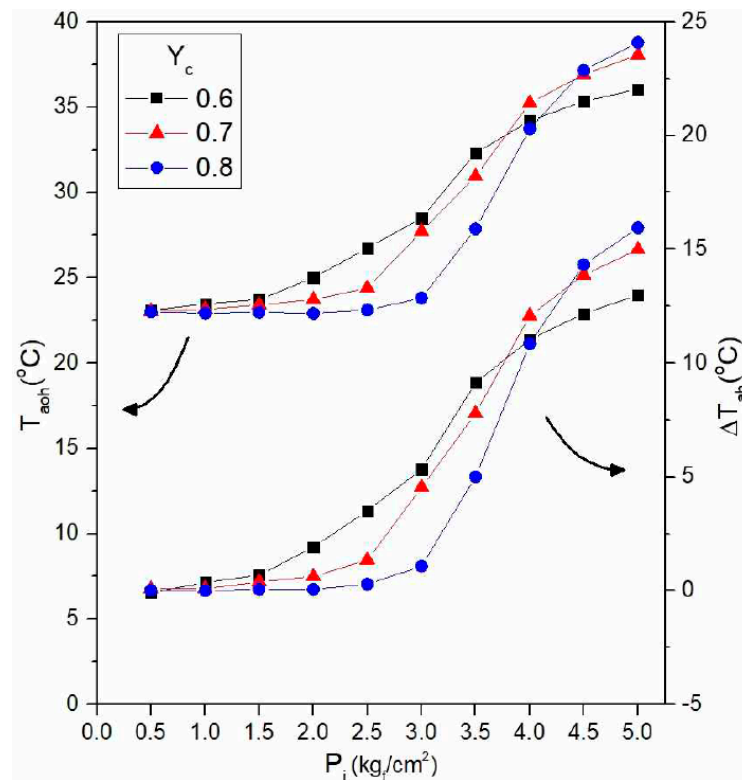


Figure 24. Indirect heat exchange method of ΔT_h according to pressure.

3.4. Temperature Control of Direct Heat Exchange Method According to Pressure

To evaluate the temperature difference with the indirect heat exchange method using the vortex tube, the supply pressure between $P_i = 0.5 \text{ kgf/cm}^2$ and $P_i = 5.0 \text{ kgf/cm}^2$ was the same as that in the basic experiment using seven nozzles for the vortex generator under the same test conditions. The inlet pressure was set at $P_i = 0.5 \text{ kgf/cm}^2$ intervals. Furthermore, as the direct heat exchange method has a larger discharge flow rate than that of the indirect heat exchange method, experiments were conducted at $y_c = 0.3$ to 0.8 for both the low-temperature type and the high-temperature type by increasing the section of the low-temperature air flow rate (y_c). To make a difference from the indirect heat

exchange method, a heater core that does heat exchange was not used. Figures 25 and 26 are the results of experiments conducted in a direct manner in which compressed air, which has undergone temperature separation, enters the chamber directly and is discharged through an air conditioning filter. Through the experiments, the value $y_c = 0.6$, which indicates the best efficiency at the exit of the low-temperature region, led to a value of T_{co} ($^{\circ}\text{C}$) = 21.76 $^{\circ}\text{C}$ when $P_i = 0.5 \text{ kgf/cm}^2$; this changed to 9.87 $^{\circ}\text{C}$ when $P_i = 5.0 \text{ kgf/cm}^2$, resulting in a maximum of 11.89 $^{\circ}\text{C}$ ΔT_{ah} ($^{\circ}\text{C}$). Through this direct heat exchange method, the low-temperature airflow ratio (y_c) did not change between the indirect and direct heat exchange methods. As a result of an experiment that involved adding $y_c = 0.3, 0.7,$ and 0.8 of T_{co} ($^{\circ}\text{C}$) in the direct heat exchange method, it was confirmed that the efficiency decreased as the pressure increased because the flow rate was insufficient in the low-temperature region, similar to the cases of $y_c = 0.6, 0.7$. It was confirmed that T_{ho} ($^{\circ}\text{C}$) produces a high-temperature region and has a resulting value similar to that of the indirect heat exchange method and similar to the value of the low-temperature region. The efficiency at T_{ho} ($^{\circ}\text{C}$) was the best at $y_c = 0.6$; when $P_i = 0.5 \text{ kgf/cm}^2$, it was 22.97 $^{\circ}\text{C}$. Additionally, when $P_i = 5.0 \text{ kgf/cm}^2$, it changed to 34.66 $^{\circ}\text{C}$ and showed a maximum temperature difference of 11.63 $^{\circ}\text{C}$. Comparing the two areas, when the ratio of the discharge flow rate became high ($y_c = 0.3$ to 0.4), it showed a trend similar to that in the basic experiment. This is because the supply pressure increases as the discharge flow rate increases in the high-temperature region, thereby increasing the flow rate discharged to the high-temperature outlet stage. Therefore, heat loss in the high-temperature chamber decreased, and the amount of temperature change decreased.

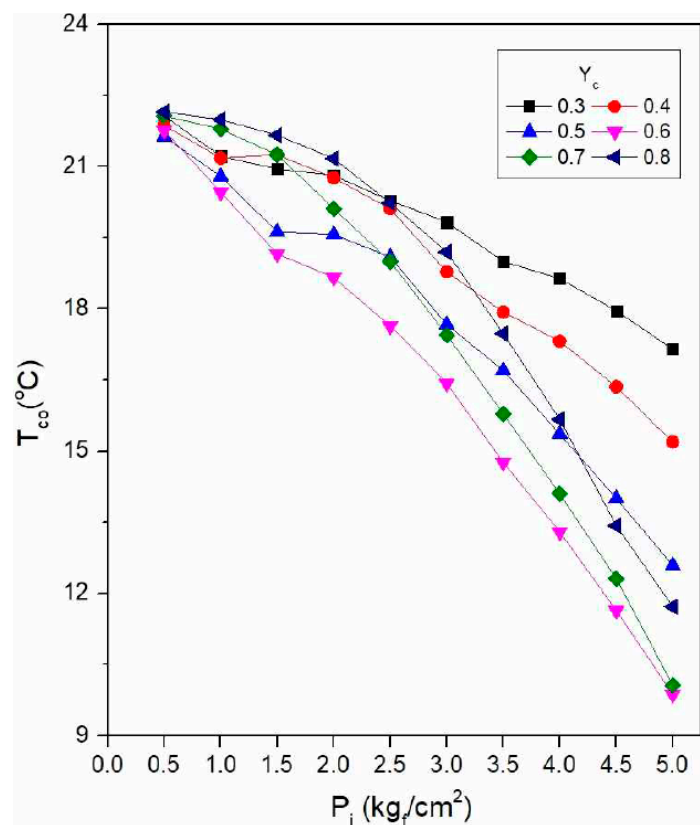


Figure 25. Direct heat exchange method of ΔT_{co} according to pressure.

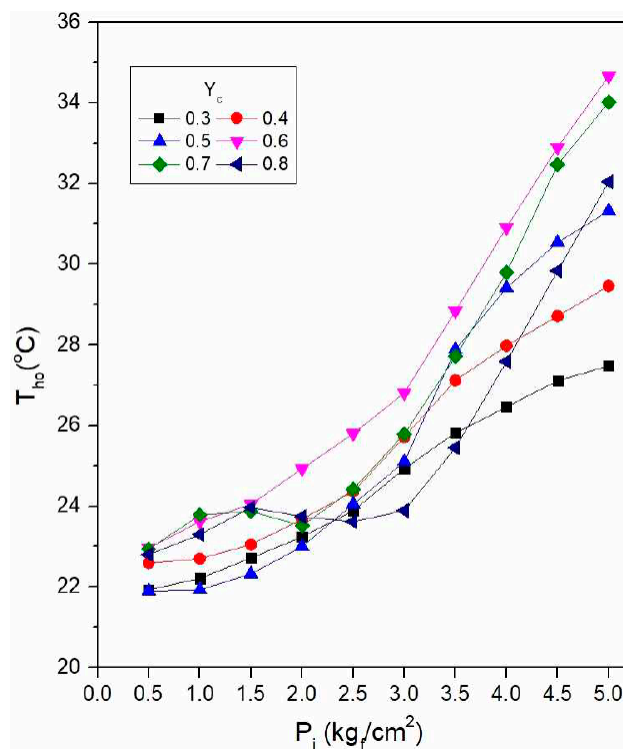


Figure 26. Direct heat exchange method of ΔT_{ho} according to pressure.

4. Conclusions

Using a vortex tube, a basic experiment was conducted to investigate the temperature separation phenomenon according to the number of nozzles of the generator according to the supply pressure (P_i) and the low-temperature air flow rate (y_c). In basic temperature difference experiments, the following conclusions were obtained using indirect and direct methods with a heater core that can be applied to a vehicle air conditioning system.

1. When the supply pressure between $P_i = 0.5 \text{ kgf/cm}^2$ and $P_i = 5.0 \text{ kgf/cm}^2$, the maximum high-temperature air temperature difference ($\Delta T_{h, \max}$) appeared at $y_c = 0.8$, and the maximum low-temperature air temperature difference ($\Delta T_{c, \max}$) appeared at $y_c = 0.5$.

2. Using 4, 5, 6, 7, and 8 nozzles in the vortex tube generator, the maximum high-temperature air temperature difference ($\Delta T_{h, \max}$) and the maximum low-temperature air temperature difference ($\Delta T_{c, \max}$) appeared for the maximum number of seven nozzles of the vortex tube generator.

3. The total discharge flow rate was tested by setting the supply pressure between $P_i = 0.5 \text{ kgf/cm}^2$ and $P_i = 5.0 \text{ kgf/cm}^2$ at intervals of $P_i = 1 \text{ kgf/cm}^2$ at the nozzle area ratio $S_n = 0.142$ (high temperature type). The discharge flow rate tended to increase in proportion to the pressure increase; and, as the number of nozzles of the generator decreased, the nozzle inner diameter (D_n) increased, resulting in four nozzles having the highest discharge flow rate.

4. In the indirect heat exchange method, efficiency was best at $y_c = 0.8$ in the high-temperature region, and at $y_c = 0.5$ in the low-temperature region.

5. According to the results of temperature measurement in the indirect heat exchange method, T_{aoc} ($^{\circ}\text{C}$) changed from $21.84 \text{ }^{\circ}\text{C}$ to $9.87 \text{ }^{\circ}\text{C}$ when the pressure was between $P_i = 0.5 \text{ kgf/cm}^2$ and $P_i = 5.0 \text{ kgf/cm}^2$ in the low-temperature region at $y_c = 0.6$ and in the high-temperature region at $y_c = 0.8$. T_{aoh} ($^{\circ}\text{C}$) showed a maximum change of $15.79 \text{ }^{\circ}\text{C}$, from $23.00 \text{ }^{\circ}\text{C}$ to $38.79 \text{ }^{\circ}\text{C}$.

6. In the direct heat exchange method, the flow rate was slower than in the indirect heat exchange method, so the discharge flow rate was large; the area of the low-temperature air flow rate (y_c) was measured at $y_c = 0.3\sim 0.8$. Excellent results were obtained in the two regions at $y_c = 0.6$. Unlike in the

indirect method, $y_c = 0.6$ was excellent at high temperature, and seems to have been affected by the discharge flow rate.

7. According to the temperature measurement results using the direct heat exchange method, when $y_c = 0.6$ and between $P_i = 0.5 \text{ kgf/cm}^2$ and $P_i = 5.0 \text{ kgf/cm}^2$, T_{co} ($^{\circ}\text{C}$) changed from $21.76 \text{ }^{\circ}\text{C}$ to $9.87 \text{ }^{\circ}\text{C}$ and its maximum difference was $11.89 \text{ }^{\circ}\text{C}$. Additionally, T_{ho} ($^{\circ}\text{C}$) showed a maximum change of $11.63 \text{ }^{\circ}\text{C}$ from $22.97 \text{ }^{\circ}\text{C}$ to $34.66 \text{ }^{\circ}\text{C}$.

To conclude this study, the temperature difference between the indirect heat exchange method and the direct heat exchange method showed a maximum value of about $4 \text{ }^{\circ}\text{C}$ in the high-temperature region; the temperature difference in the low-temperature region was insignificant. Although the indirect heat exchange method looks slightly better when comparing the time to reach normal temperature, the indirect heat exchange method takes about four times longer than the direct heat exchange method, and the direct heat exchange method seems to have an excellent reaction speed. This is because the use of an indirect heat exchange type heater core induces flow velocity resistance, and the heat exchange of the heater core is performed only with air. However, when applied to an air conditioning system, the indirect heat exchange method, using external air or internal air, can implement a filter to reduce foreign substances; however, in the direct method, compressed air can be filtered only through the air conditioning filter. It is thought that it may be necessary to solve this problem. Therefore, for a vehicle air conditioning system, a direct heat exchange method with low reaction speed and low flow resistance can be used and, in the case of low-temperature airflow ratio (y_c), a value of $y_c = 0.6$, with high efficiency in both the low temperature and high-temperature regions, will subsequently be used in the air conditioning system of an eco-friendly vehicle. It is judged that this system can be applied and used effectively.

Author Contributions: All authors contributed to this research in collaboration. Y.K. have an experiment, S.I. proposed the conceptualization, and J.H. provided substantial help with the paper schedule and implemented the proposed vehicle air conditioning system using vortex tube. All authors have read and agreed to the published version of the manuscript.

Funding: This research received no external funding.

Acknowledgments: This work was supported by the National Research Foundation of Korea (NRF) grant funded by the Korean government (MSIT) (no. NRF-2019R1G1A1100739).

Conflicts of Interest: The authors declare no conflict of interest.

Nomenclature

A	The rate of vortex flow coming inside [L/min]
c	Constant
D	The inner diameter of the vortex tube [mm]
d_c	The diameter of cold end orifice [mm]
D_n	The inner diameter of nozzles [mm]
L	Tube length [mm]
P_i	The pressure of inlet air [kgf/cm^2]
Q	Mean air flow rate [L/min]
S_n	Nozzle area ratio (nozzle sectional area/vortex tube sectional area [-])
T	Static temperature [K]
ΔT_{ac}	The temperature difference between inlet air and cold outlets air for chamber [$^{\circ}\text{C}$] ($\Delta T_{ac} = T_{aoc} - T_{ai}$)
ΔT_{ah}	The temperature difference between inlet air and hot outlets air for chamber [$^{\circ}\text{C}$] ($\Delta T_{ah} = T_{aoh} - T_{ai}$)
T_{aoc}	The temperature of outlets cold air for chamber [$^{\circ}\text{C}$]
T_{aoh}	The temperature of outlets hot air for chamber [$^{\circ}\text{C}$]
T_c	The temperature of cold air [$^{\circ}\text{C}$]
ΔT_c	The temperature difference between inlet air and cold air [$^{\circ}\text{C}$] ($\Delta T_c = T_c - T_o$)

$\Delta T_{c, \max}$	The maximum temperature difference between inlet air and cold air [$^{\circ}\text{C}$]
T_{co}	The temperature of cold outlet air for after passing the fan [$^{\circ}\text{C}$]
T_h	The temperature of hot air [$^{\circ}\text{C}$]
ΔT_h	The temperature difference between inlet air and hot air [$^{\circ}\text{C}$] ($\Delta T_h = T_h - T_o$)
$\Delta T_{h, \max}$	The maximum temperature difference between inlet air and hot air [$^{\circ}\text{C}$]
T_{ho}	The temperature of hot outlet air for after passing the fan [$^{\circ}\text{C}$]
T_{ai}	The temperature of inlet air for chamber [$^{\circ}\text{C}$]
$\Delta T_{w, \max}$	The maximum temperature difference between inlet air and hot wall [$^{\circ}\text{C}$]
y_c	Cold air mass flow ratio (cold air mass flow/inlet air mass flow)
w	Angular velocity [L/s]
r	Diameter radial direction

Subscript

c	Cold air
h	Hot air
I	Inlet air
max	Maximum
N	Nozzle and number

References

- Jetter, J. Evaluation of Alternatives for HFC-134a Refrigerant in Motor Vehicle Air Conditioning. In Proceedings of the International Conference on Ozone Protection Technologies, Washington, DC, USA, 21–23 October 1996; pp. 845–854.
- Global Environmental Change Report, A Brief Analysis of the Kyoto Protocol. December 1997, Volume IX. No. 24. Available online: <https://www.oecd.org/dev/1923191.pdf> (accessed on 7 October 2020).
- Linderstrøm-Lang, C. Gas separation in the Ranque-Hilsch vortex tube. *Int. J. Heat Mass Transf.* **1964**, *7*, 1195–1206. [[CrossRef](#)]
- Ranque, G.J. Experiments on expansion in a vortex with simultaneous exhaust of hot air and cold air. *Phys. Radium* **1933**, 112–114.
- Hilsch, R. The Use of the Expansion of Gases in a Centrifugal Field as Cooling Process. *Rev. Sci. Instr.* **1947**, *18*, 108–113. [[CrossRef](#)] [[PubMed](#)]
- Fulton, C.D. Ranque's Tube. *Refriger. Eng.* **1950**, *5*, 473–479.
- Stephan, K.; Lin, S.; Durst, M.; Huang, F.; Seher, D. An investigation of energy separation in a vortex tube. *Int. J. Heat Mass Transf.* **1983**, *26*, 341–348. [[CrossRef](#)]
- Deissler, R.; Perlmutter, M. Analysis of the flow and energy separation in a turbulent vortex. *Int. J. Heat Mass Transf.* **1960**, *1*, 173–191. [[CrossRef](#)]
- Kassner, R.; Knoernschild, E. *Friction Laws and Energy Transfer in Circular Flow*; Wright Patterson Air Force Base: Montgomery County, OH, USA, 1948; p. 259.
- Behera, U.; Paul, P.; Kasthuriangan, S.; Karunanithi, R.; Ram, S.; Dinesh, K.; Jacob, S. CFD analysis and experimental investigations towards optimizing the parameters of Ranque–Hilsch vortex tube. *Int. J. Heat Mass Transf.* **2005**, *48*, 1961–1973. [[CrossRef](#)]
- Gao, C.M.; Bosschaart, K.J.; Zeegers, J.C.H.; de Waele, A.T.A.M. Experimental study on a simple Ranque-Hilsch vortex tube. *Cryogenics* **2005**, *45*, 173–183. [[CrossRef](#)]
- Westley, R. The College of Aeronautics (Cranfield) Note, No. 30(1955-5): No. 67(1957-7). Available online: <https://www.cambridge.org/core/journals/aeronautical-journal/article/research-at-the-college-of-aeronautics-cranfield/E5F9971CA8C27168C0349632BF1AA963> (accessed on 7 October 2020).
- Hatnett, J.P.; Eckert, E.R.G. Experimental Study of the Velocity and Temperature Distribution in a High Velocity Vortex-type Flow. *Trans. ASME* **1957**, *79*, 751–758.
- Takahama, H. Studies on Vortex Tubes (2nd Report), Reynolds Number the Effect of the Cold Air Rate and the Partial Admission of Nozzle on the Energy Separation. *Bull. JSME* **1996**, *9*, 121–130. [[CrossRef](#)]
- Comasser, S. The Vortex tube. *J. AM. Soc. Naval Eng.* **1951**, *63*, 99–108. [[CrossRef](#)]

16. Stephan, K.; Lin, S.; Durst, M.; Huang, F.; Seher, D. A similarity relation for energy separation in a vortex tube. *Int. J. Heat Mass Transf.* **1984**, *27*, 911–920. [[CrossRef](#)]
17. Fröhlingdorf, W.; Unger, H. Numerical investigations of the compressible flow and the energy separation in the Ranque–Hilsch vortex tube. *Int. J. Heat Mass Transf.* **1999**, *42*, 415–422. [[CrossRef](#)]
18. Eiamsa-Ard, S.; Promvong, P. Numerical investigation of the thermal separation in a Ranque–Hilsch vortex tube. *Int. J. Heat Mass Transf.* **2007**, *50*, 821–832. [[CrossRef](#)]
19. Skye, H.M.; Nellis, G.F.; Klein, S.A. Comparison of CFD analysis to empirical vortex tube. *Int. J. Refrig.* **2006**, *29*, 71–80. [[CrossRef](#)]
20. Kaya, H.; Uluer, O.; Kocaoğlu, E.; Kirmaci, V. Experimental analysis of cooling and heating performance of serial and parallel connected counter-flow Ranque–Hilsch vortex tube systems using carbon dioxide as a working fluid. *Int. J. Refrig.* **2019**, *106*, 297–307. [[CrossRef](#)]
21. Li, N.; Jiang, G.; Fu, L.; Tang, L.; Chen, G. Experimental study of the impacts of the cold mass fraction on internal parameters of a vortex tube. *Int. J. Refrig.* **2019**, *104*, 151–160. [[CrossRef](#)]
22. Hu, Z.; Li, R.; Yang, X.; Yang, M.; Day, R.; Wu, H.-W. Energy separation for Ranque-Hilsch vortex tube: A short review. *Therm. Sci. Eng. Prog.* **2020**, *19*, 100559. [[CrossRef](#)]
23. Rafiee, S.E.; Sadeghiazad, M.M. Experimental analysis on the impact of navigator’s angle on velocimetry and thermal capability of RH-vortex tube. *Appl. Therm. Eng.* **2020**, *169*, 114907. [[CrossRef](#)]
24. Fotso, B.M.; Talawo, R.; Nguefack, M.F.; Fogue, M. Modeling and thermal analysis of a solar thermoelectric generator with vortex tube for hybrid vehicle. *Case Stud. Therm. Eng.* **2019**, *15*, 100515. [[CrossRef](#)]
25. Thakare, H.; Parekh, A.D. Experimental investigation of Ranque–Hilsch vortex tube and techno–Economic evaluation of its industrial utility. *Appl. Therm. Eng.* **2020**, *169*, 114934. [[CrossRef](#)]
26. Dutta, T.; Sinhamahapatra, K.; Bandyopadhyay, S.S. CFD Analysis of Energy Separation in Ranque-Hilsch Vortex Tube at Cryogenic Temperature. *J. Fluids* **2013**, *2013*, 1–14. [[CrossRef](#)]
27. Im, S.Y. An Experimental Study on the Geometric setup of a Low-Pressure Vortex tube. Master’s Thesis, Chungnam National University, Daejeon, Korea, 2004.



© 2020 by the authors. Licensee MDPI, Basel, Switzerland. This article is an open access article distributed under the terms and conditions of the Creative Commons Attribution (CC BY) license (<http://creativecommons.org/licenses/by/4.0/>).